

Full-depth Flexible Pavement Fatigue Response under Various Tire and Axle Load Configurations

Hao Wang¹ and Imad L. Al-Qadi²

ABSTRACT:

The goal of this study was to evaluate the effect of vehicle parameters, mainly tire configuration and axle load, on full-depth flexible pavement response using accelerated pavement testing. The Advanced Transportation Loading ASsembly (ATLAS), housed at the University of Illinois at Urbana-Champaign, was used in this study. The tests were performed on three full-depth flexible pavement sections of 152, 254 and 429mm HMA placed on 300mm of lime-stabilized subgrade. The test program included three tire types (dual-tire assembly, wide-base 425 tire, and wide-base 455 tire); five loading levels (26, 35, 44, 53, and 62kN); three tire inflation pressures (550, 690, and 760kPa); and two speeds (8 and 16km/h). The measured longitudinal strain at the bottom of the HMA was compared under various loading conditions.

The study concluded that the wide-base 425 tire, which was originally introduced for pavement testing only, exhibited the highest fatigue potential caused by high tensile strain at the bottom of HMA; while the dual-tire assembly exhibited the lowest tensile strain at the bottom of HMA. However, the difference in strain responses due to wide-base tires and dual-tire assembly diminishes as HMA thickness increases. The effect of load on fatigue life is expressed as an exponential function. The load damage exponents were found to be in the range of 1.77-3.29 for full-depth flexible pavement. The parameter was found to depend on pavement thickness and tire configuration. However, the authors believe that near-surface cracking caused by shear is more critical than tensile strain at the bottom of HMA for perpetual pavements.

Keywords: Accelerated Pavement Testing, Full-depth Flexible Pavement, Fatigue, Tire and Axle Load

Conference Topic Selected: Modeling and analysis of pavement systems

Submission Date: March 14, 2008

¹ Graduate Research Assistant, Department of Civil and Environmental Engineering, University of Illinois at Urbana-Champaign, 205 N Mathews MC-250, Urbana, IL 61801, E-mail: haowang4@uiuc.edu

² **Corresponding Author**, Founder Professor of Engineering, Illinois Center for Transportation, Director, University of Illinois at Urbana-Champaign, 205 N Mathews MC-250, Urbana, IL 61801, E-mail: alqadi@uiuc.edu

1. Introduction

The amount of damage caused by truck traffic greatly depends on truck loading, pavement structure, and the environment. The factors related to truck loading can be classified into two major components: the vehicle generating the load and the axle and tire configuration transferring the load. To better characterize the pavement damage induced by truck loading, the effects of tire loading, tire inflation pressure, vehicle speed, and tire configuration on the pavement response must also be considered.

Accelerated pavement testing (APT) provides an acceptable solution between real field pavement loading and laboratory tests to evaluate the effect of truck loading parameters on pavement damage. Accelerated pavement testing compresses many years of pavement load-related deterioration into just a few months or weeks of testing. During the accelerated pavement testing, the pavement response to loading can be measured using pavement instrumentation. The parameters that can be measured include strains, stresses, deflections, moisture, temperature, etc. In-situ measurements of these parameters allow for the development of accurate performance models and the calibration of mechanistic pavement design approaches (1).

Recently, various accelerated pavement testing projects have been conducted to measure realistic pavement responses: Penn State Test Track (2), MnRoad (3), WesTrack (4), and the Virginia Smart Road (5). However, the main focus of each project was somewhat different. For instance, the Penn State project focused on determining layer moduli and evaluating mechanistic distress models, while the initial interest of the MnRoad was assessing existing pavement design models and developing new transfer functions. The Westrack project team's interest was the evaluation of hot-mix asphalt (HMA) performance, as opposed to pavement design evaluation. The Virginia Smart Road's main objectives were to calibrate falling weight deflectometer (FWD) measurements, evaluate different SuperPaveTM mix performances and durability, calibrate and optimize ground penetrating radar (GPR) for measuring layer thicknesses and detecting flaws in pavements, as well as measuring the response of different pavement designs to various loading characteristics.

This paper focuses on the pavement responses under various loading characteristics applied through accelerated pavement testing. The considered loading parameters included three tire types (dual-tire assembly, wide-base 425 tire, and wide-base 455 tire); five loading levels (26, 35, 44, 53, and 62kN); three tire inflation pressures (550, 690, and 760kPa); and two speeds (8 and 16km/h). The paper presents the measured horizontal tensile strains induced by various loading conditions under the three full-depth HMA layer thicknesses and analyzes the effects of tire configuration, axle load, vehicle speed, and tire pressure on the measured strains and pavement fatigue damage.

2. Full-depth Pavements and Instrumentation

2.1 Test Sections

The experimental program made use of existing HMA test sections built as part of an extended-life pavement project (6). These sections included various full-depth HMA pavement designs that are widely encountered on high priority routes. The full-depth

asphalt pavement is composed of HMA layers directly over a lime-stabilized subgrade. The test sections included three HMA thicknesses: 152, 254, and 420mm. Figure 1 shows the layout and cross sections of the test sections.

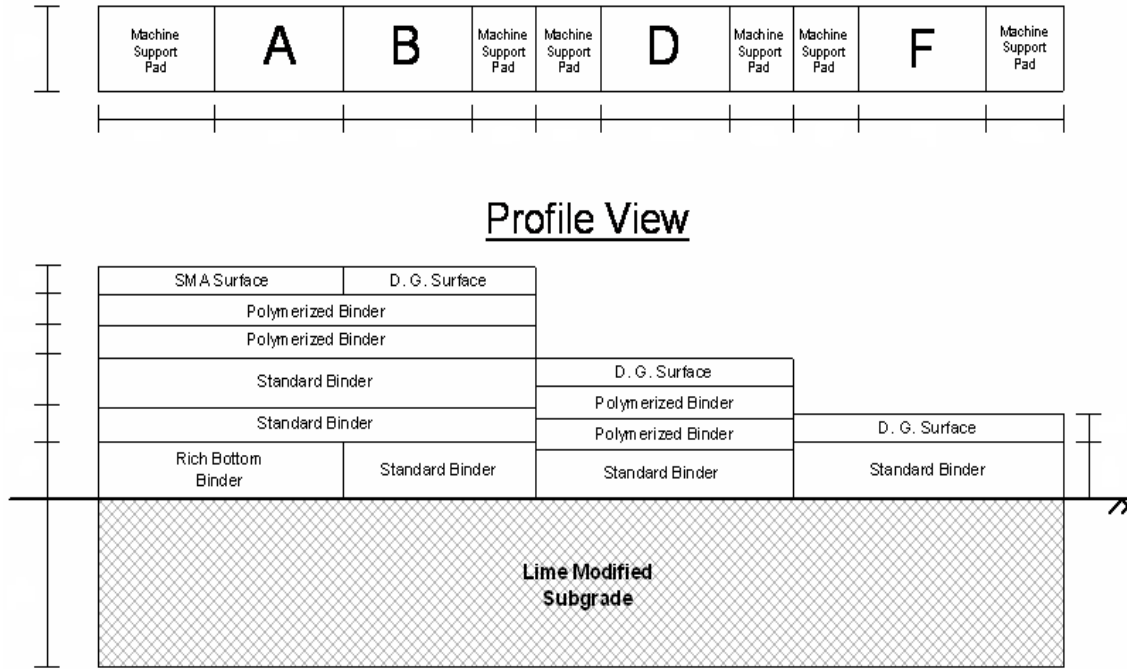


FIGURE 1 General layout of the full-depth HMA pavement test sections.

The HMA was prepared in accordance with the Superpave™ volumetric design procedure. The laboratory mix-design criterion is based on 90 gyrations to achieve 4% air void (2.5% for rich bottom binder course); N85 for Stone Matrix Asphalt (SMA). Three asphalt binders were used in the HMA layers, a PG 64-22 for standard binder and rich bottom binder courses, a SBS PG 70-22 for polymer modified binder courses and dense graded surface, and a SBS PG 76-28 for SMA surface course. The asphalt contents of the standard and polymer modified binder and rich bottom binder courses are 4.5% and 5.1%, respectively; while the dense-graded and SMA asphalt content is 5.4%. No liquid anti-strips were used in any mixture. The aggregate used in all mixes is limestone; however, steel slag was used as coarse aggregate in SMA. The subgrade is lime-stabilized to address the high water content existing in the nature soil.

2.2 Pavement Instrumentation

One of the most critical responses considered in flexible pavements is the horizontal strain at the bottom of the HMA layer. Longitudinal and transverse strain measurements were obtained at the stabilized subgrade-HMA interface using an H-shape strain gauge. The strain gauge has a 120Ω resistance with a gauge factor of 2 and can measure up to 2000 microstrains. Three strain gauges were placed along the centerline of each test section, at approximately the center of the section. Two of the gauges were placed laterally, and the third was placed longitudinally. These gauges were embedded in a thin

3.6m
1.5m
5.0m
5.7cm
5.7cm

layer of polymer modified mix that was scalped to produce a sand size mix. Temperature data was continuously collected using thermocouples throughout the pavement depth. The strain gauges and thermocouple instruments were connected to a Labview data acquisition system.

3. Experiment Program

3.1 Accelerated Testing Loading ASsembly (ATLAS)

The accelerated pavement testing facility used in this study was the Accelerated Testing Loading ASsembly (ATLAS), which is a linear full-scale simulator of traffic loading housed at the Advanced Transportation Research and Engineering Laboratory (ATREL) facility at the University of Illinois at Urbana-Champaign. The system is capable of simulating truck, aircraft, and rail traffic loading; the detailed characteristics of ATLAS are listed in Table 1.

Table 1 ATLAS Characteristics

| | |
|------------------------------------|---|
| Weight (kN) | 694 |
| Dimensions (m) | 37.8 x 3.7 x 3.7 |
| Load capacity (kN) | 356 |
| Tire load rating (kN) | Dual-tire assembly: 53.4 Wide-base tire: 62.3 Aircraft tire: 222 |
| Traffic length (m) | 26 (length of constant speed is 20m) |
| Max wheel speed (km/h) | 16 |
| Loading conditions | Uni- or Bi-directional Adjusted lateral position, fixed or distributed |
| Maximum tire transverse offset (m) | 1.0 |

ATLAS is mounted on four crawler tracks and can be moved from one pavement test section to another when testing is completed. During operation, ATLAS is supported on four columns at the end spans and transmits loads to the pavement structure through a hydraulic ram attached to a wheel carriage, which can accommodate a single tire, dual tires, and aircraft tires. A winch motor is used to pull the wheel carriage back and forth on the test section without gear. Figure 2 shows the ATLAS system with testing tires. A personal computer, housed in an adjacent trailer, is used to operate ATLAS. Another nearby mechanical equipment trailer houses the necessary electrical and mechanical equipment.



FIGURE 2 Advanced Transportation Loading ASsembly (ATLAS) with (a) dual-tire assembly; and (b) wide-base tire.

3.2 Tire Configurations

Tire size, structure composition (rubber and reinforcement), and inflation pressure are important tire characteristics for carrying the load. Three tire configurations were selected for applying load in this study: wide-base 455, wide-base 425, and 11R22.5 dual-tire assembly. The 11R22.5 dual-tire is widely used in commercial trucks. The wide-base 425 tire was originally designed for pavement testing only, and the wide-base 455 tire is the second-generation of wide-base tires. Wide-base tires are proposed to be used on the non-steering axles to replace the traditional dual-tire assembly or used on high-load steering axles for better load distribution (7). Wide-base tires typically range from 400 to 460mm in width as opposed to the 250 to 305mm width for typical radial truck tires.

The detailed dimensions of the tires used in this study are summarized in Table 2. The nomenclature of tires includes three tire dimensions and type of tire in the form of AAA/BBXCC.C. The first number (AAA) is the tire width from wall-to-wall in mm/in, the second number (BB) is the side wall height given as a percentage of the tire width, the letter (X) indicates the type of tire (radial or bias ply), and the third number (CC.C) is the tire rim diameter in inches. For example, a tire designation 455/55R22.5 is a radial tire (indicated with the ‘R’), has a wall-to-wall width of 455mm, a wall height of 250mm, and a rim diameter of 571.5mm.

Table 2 Dimensions of Dual and Wide-base Tires Used in the Test

| Tire type | Loaded Radius (mm) | Overall Diameter (mm) | Overall width (mm) | Tread depth (mm) |
|----------------|--------------------|-----------------------|--------------------|------------------|
| Dual 11R22.5 | 488 | 1049 | 285 | 22 |
| WB-425/65R22.5 | 522 | 1130 | 421 | 18 |
| WB-455/55R22.5 | 498 | 1078 | 448 | 22 |

3.3 Testing Matrix

The tire loading was conducted uni-directionally to simulate vehicular field loading conditions. The loading parameters considered in this study were five wheel loads, three tire pressures, two speeds, and three tire configurations, as presented in Table 3. Hence, 90 loading combinations were applied to measure pavement responses; each applied for 20 passes. The tensile strains were recorded at a rate of 100Hz. The average peak values of the tensile strains for each 20 passes were determined. The pavement temperatures were recorded at each pass and stored in a separate text file. An in-house software based on Excel VBA was developed and used to organize and analyze the data efficiently.

Table 3 Test Matrix for Various Tire Configurations

| Tire load (kN) | Speed (km/h) | Tire pressure (kPa) | Tire configuration | Offsets (mm) |
|---------------------------|-----------------|------------------------|--|--|
| 26, 35, 44, 53 & 62 | 8, 16 | 550, 690 & 760 | Dual, Wide- base 455 & Wide-base 425 | Dual: 0, 150 & 250 Wide-base 455: 0 & 178 Wide-base 425: 0 & 165 |

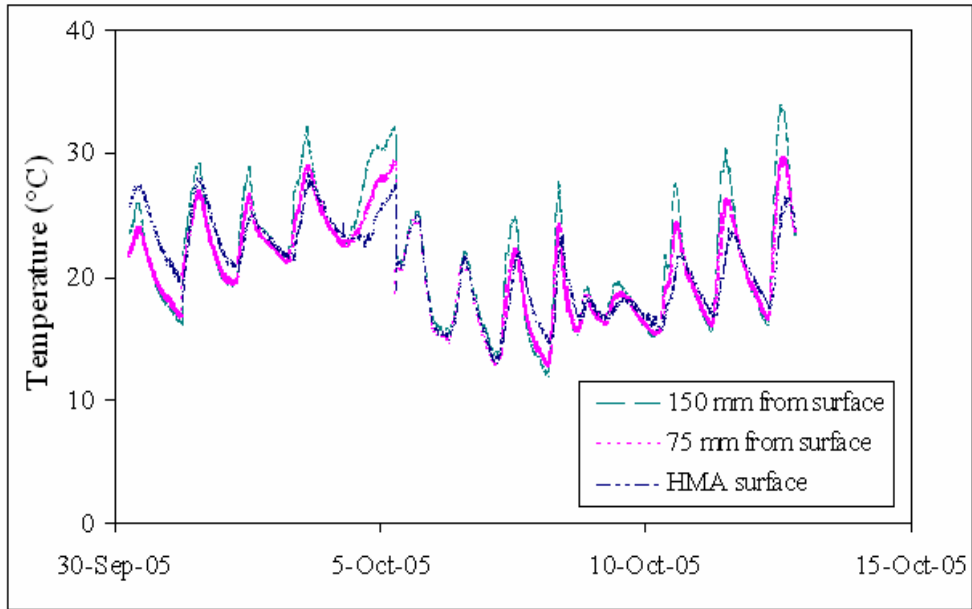
4. Results and Analysis

4.1 Temperature Correction of Measured Strain

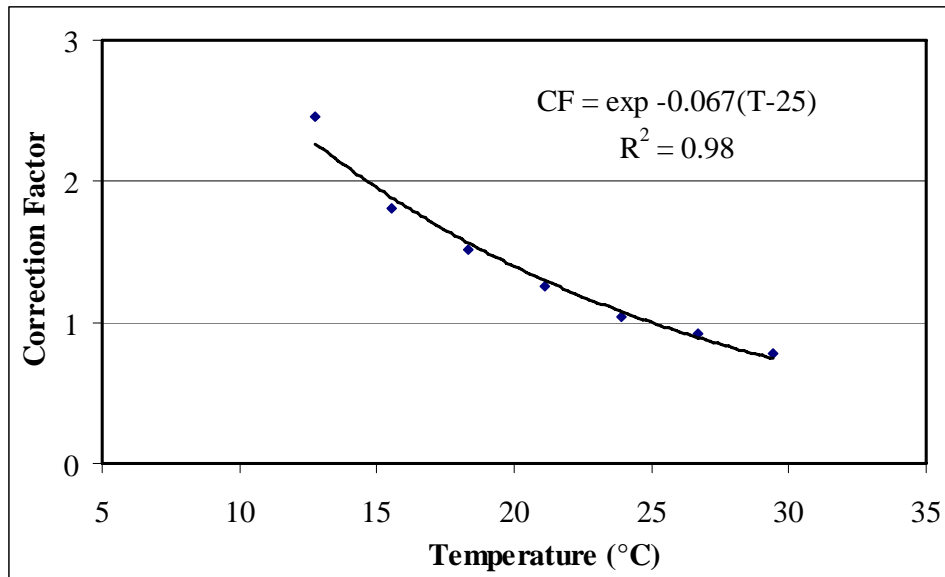
The temperature at various depths of the HMA layer was recorded during the testing and tabulated with the corresponding strains. Figure 3 (a) shows that temperatures varied significantly throughout the testing period, 11-34°C for section F; with up to 5°C difference within the pavement structure. This difference was greater for thicker sections. The mean temperature of the measurements from thermocouples throughout the HMA layer was used as testing temperature in the analysis.

The collected strains were shifted to a reference temperature 25°C, to allow comparison between the responses due to various tire configurations. Tests were first repeated at various times of the day, under the same loading conditions. Collected strain data were used to develop an exponential regression model with respect to testing temperature (5). The correction factor (CF) was then obtained using Equation 1. The raw measurements were then multiplied by the CF to get the corrected responses at reference temperature. An example of temperature correction factor for section F is shown in Figure 3(b). The strains after temperature correction were used for comparison under various tire and axle load configurations in this paper.

$$\text{Correction Factor} = \frac{\text{response at reference temperature (25}^\circ\text{C)}}{\text{response at testing temperature}} \quad (1)$$



(a)



(b)

FIGURE 3 (a) Temperature profile through the HMA layer and (b) temperature correction factor for section F.

4.2 Dynamic Strain Responses

The measured dynamic longitudinal and transverse strain pulses for dual-tire assembly at section D (16km/h speed, 35kN load, and 690kPa inflation pressure, at 25°C) is shown in Figure 4. The strain pulse clearly demonstrates the viscoelastic behavior of HMA: relaxation with time and asymmetry of the response.

As expected, the longitudinal strain was composed of a compressive part followed by a tensile part. This may be explained as follows: When the tire moves towards the longitudinal strain gauge, tension results directly beneath the tire and compresses at the gauge location due to bending and compression shear resulting from the wheel traction with HMA surface. Hence, compression strain is developed at the strain gauge location. When the tire is directly above the strain gauge, bending tension took place with no shear. As the tire moves away from the gauge, compression bending and shear tension due to surface-tire traction results, which may be balanced to zero. On the other hand, the transverse strain is composed of only a tensile part. The tension increases when the tire approaches the transverse strain gauge, which means more load was distributed on the gauge location. Thus, a relatively longer tensile time period is spent during the transverse strain compared to the longitudinal strain.

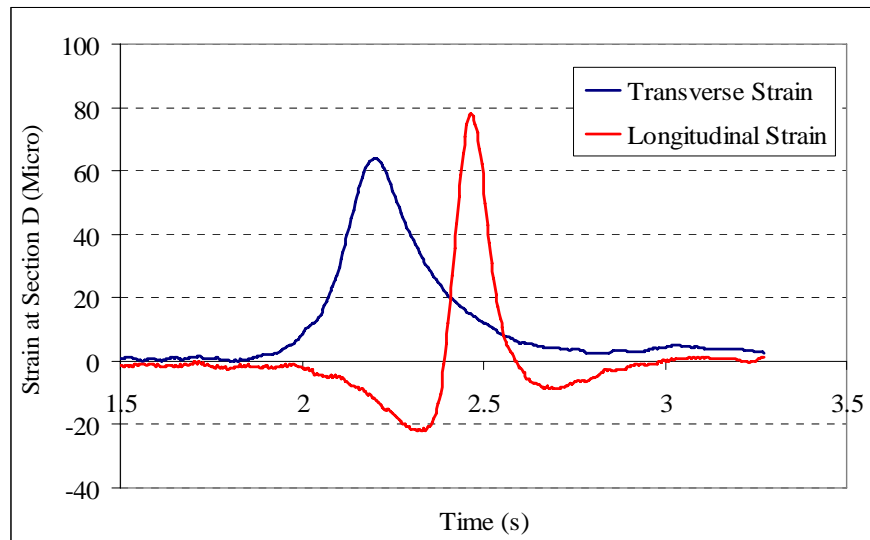
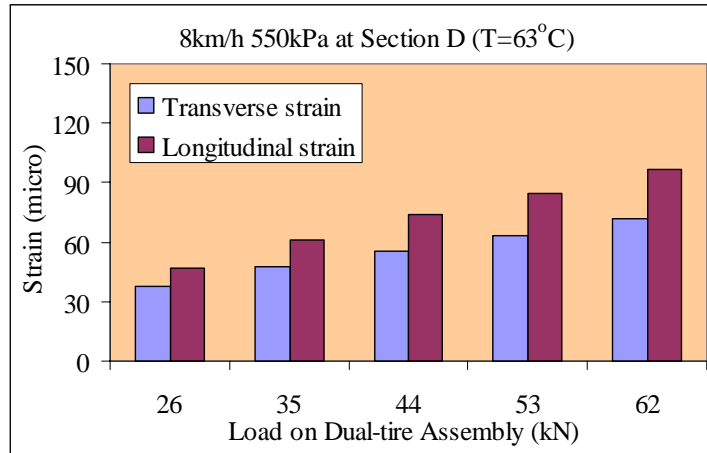


FIGURE 4 Measured transverse and longitudinal strains at the bottom of HMA at section D under one tire center of dual-tire assembly.

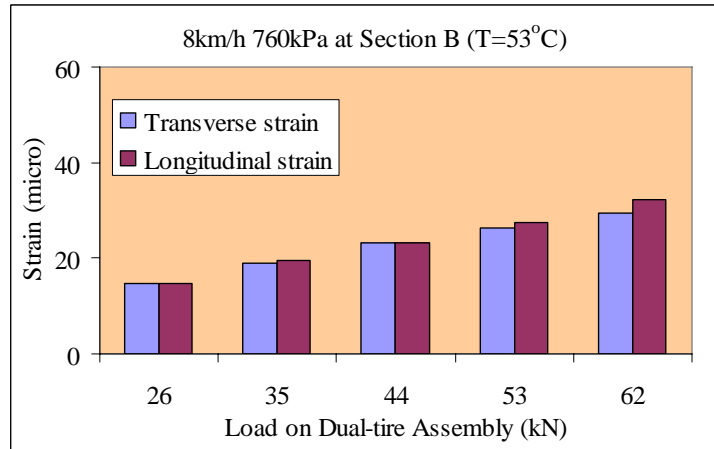
The maximum strain, which is defined as the difference between the peak response and zero, is calculated under various loading conditions. As expected, the maximum longitudinal and transverse tensile strains are located directly under the center of single wide-base tire. However, for dual-tire assembly, the maximum transverse tensile strain is located under one tire center and the longitudinal tensile strain under the center of dual-tire assembly is similar to that under one tire center.

The measured maximum transverse and longitudinal tensile strains at section D and B (The transverse strain gauges were not functional at testing for section F) are shown in Figures 5 (a), (b), (c), and (d), respectively for dual-tire assembly and wide-base 455 tire. It is clearly shown that the longitudinal strains are greater than the transverse strains under the dual-tire assembly. The difference diminishes as the pavement thickness increases. This is consistent with previous findings (7). For the wide-base tire, the transverse strains are similar to, or a little greater than, the longitudinal strains due to the single tire loading. In addition to the aforementioned, the longitudinal strain is less affected than the transverse strain by the relative distance between the tire center and

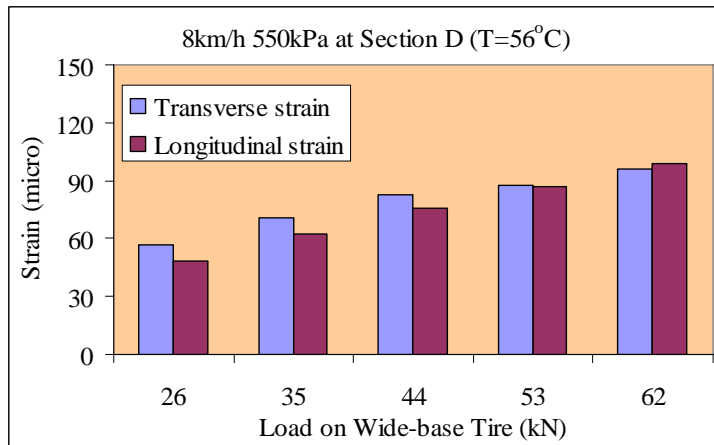
strain gauge location; hence, the longitudinal strain was selected as the critical strain for bottom-up fatigue cracking.



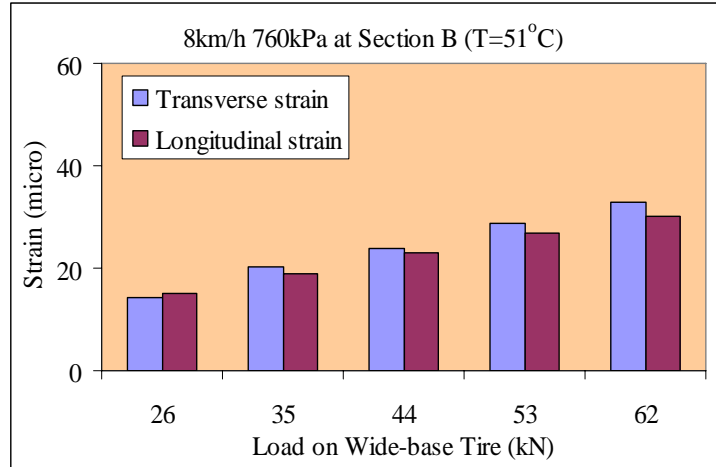
(a)



(b)



(c)

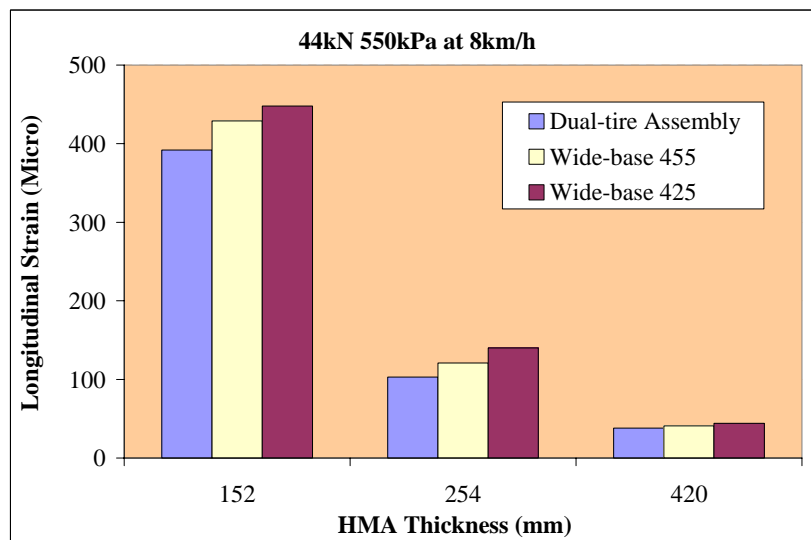


(d)

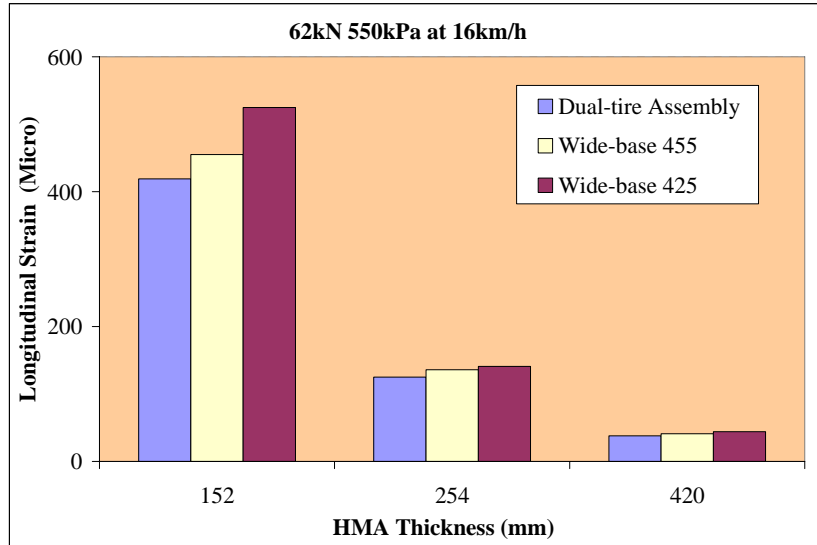
FIGURE 5 Comparison of measured transverse and longitudinal strains for (a) dual-tire assembly at section D, (b) dual-tire assembly at section B, (c) wide-base 455 tire at section D, and (d) wide-base 455 tire at section B

4.3 Comparison of Longitudinal Strains for Different Tire Configurations

The measured longitudinal strains under wide-base 425 and 455 tires at the three sections were compared with the longitudinal strains under conventional dual-tire assembly, Figure 6. The results showed that the wide-base 425 tire, which is originally introduced for pavement testing only, exhibited the greatest bottom-up fatigue potential caused by high tensile strain at the bottom of HMA; while dual-tire assembly exhibited the lowest tensile strain at the bottom of HMA. However, the difference in strain responses due to wide-base tires and dual-tire assembly diminished as HMA thickness increased. When the HMA thickness is equal or greater than 420mm, the effect of tire size becomes negligible.



(a)



(b)

FIGURE 6 Measured strains under various tire configurations for (a) 44kN and 8km/h and (b) 62kN and 16km/h.

The calculated relative ratios for the two wide-base tires with respect to dual-tire assembly at 8km/h and 16km/h are shown in Table 4. The 455 wide-base tire resulted in an average of 16% higher critical strain response at the bottom of the HMA layer than conventional dual-tire assembly under the same test configurations (speed, wheel load, inflation pressure, and pavement structure), compared to an average 25% increase when the wide-base 425 tire is used. It has to be noted that these differences, especially between the wide-base 455 and dual-tire assembly, diminish as HMA thickness increases.

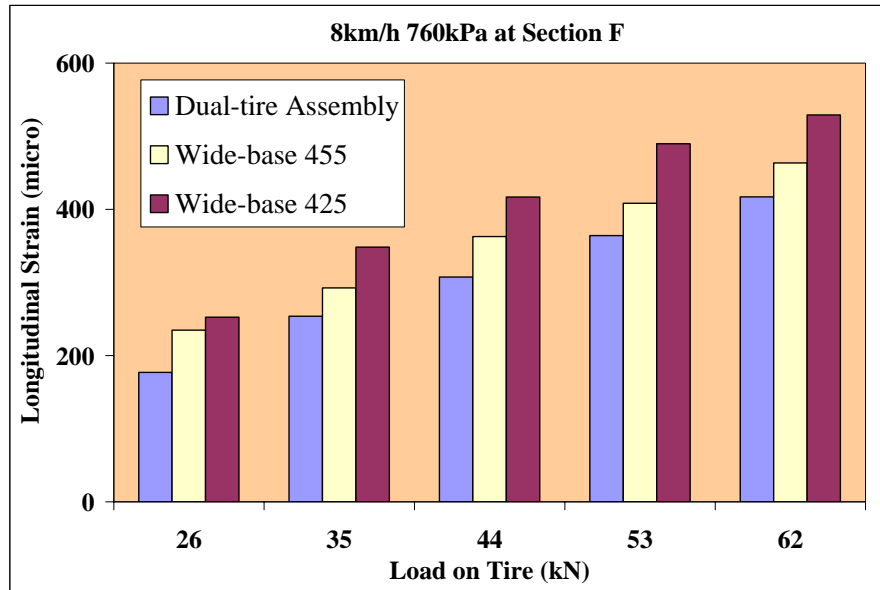
Table 4 Relative Strain Ratios between Wide-base Tires and Dual-tire Assembly

| Speed (km/h) | 8 | | | 16 | | |
|--------------|---------|--------------------|-----------|---------|--------------------|-----------|
| | Average | Standard deviation | Range | Average | Standard deviation | Range |
| W425 | 1.25 | 0.1 | 1.06-1.44 | 1.26 | 0.08 | 1.12-1.47 |
| W455 | 1.16 | 0.09 | 1.01-1.4 | 1.17 | 0.06 | 1.06-1.35 |

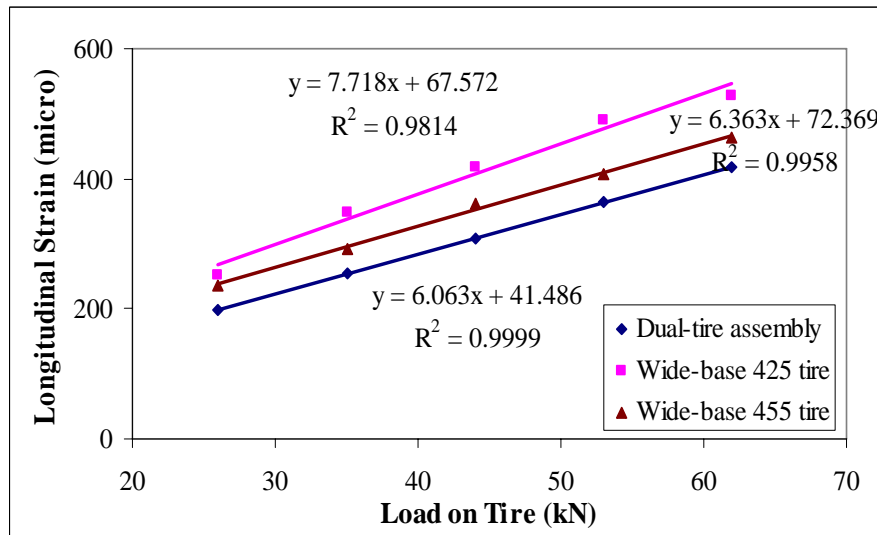
4.4 Effect of Wheel Load

Highway traffic consists of an array of vehicles with various weights and axle configurations. The measured strain response under different wheel loads from 26kN to 62kN at 8km/h and 690kPa tire pressure for section F are plotted in Figure 7. As would

be expected, the longitudinal strain responses increase linearly with the load regardless of tire configurations.



(a)



(b)

FIGURE 7 Measured strains under different wheel loads at section F.

The effect of overweight truck loading was evaluated using the load equivalence factor (LEF) in terms of the damage it causes. The load damage exponent (n) was calculated as the exponent between the ratio of damage life and the ratio of load magnitudes, Equation 2 (8).

$$LEF = N_i / N_j = (P_j / P_i)^n \quad (2)$$

where,

LEF = load equivalency factor for the fatigue damage;

P_i = magnitude of load;

N_i = number of loads with magnitude P_i to cause failure; and

n = load damage constant for the specific structure distress.

The measured longitudinal tensile strains at the bottom of HMA under various axle load levels were incorporated into the fatigue equation used in the proposed AASHTO 2002 Mechanistic Empirical Pavement Design Guide (MEPDG) (9). The calculated load damage exponents for dual-tire assembly and wide-base tires were compared in Figure 8 for various HMA thicknesses. The average load damage constants for various loads with respect to the reference load (44kN) are presented; the error bar indicates the standard deviation of these load damage exponents. The range of load damage exponents is 1.77–3.29 for all sections. Generally, the load damage exponents decrease with pavement thickness increase. This suggests that if the axle load is increased by 10%, the fatigue damage would increase by 18% for section A and 37% for section F. It was also found that the wide-base 455 tire had smaller load damage exponents than the dual-tire assembly.

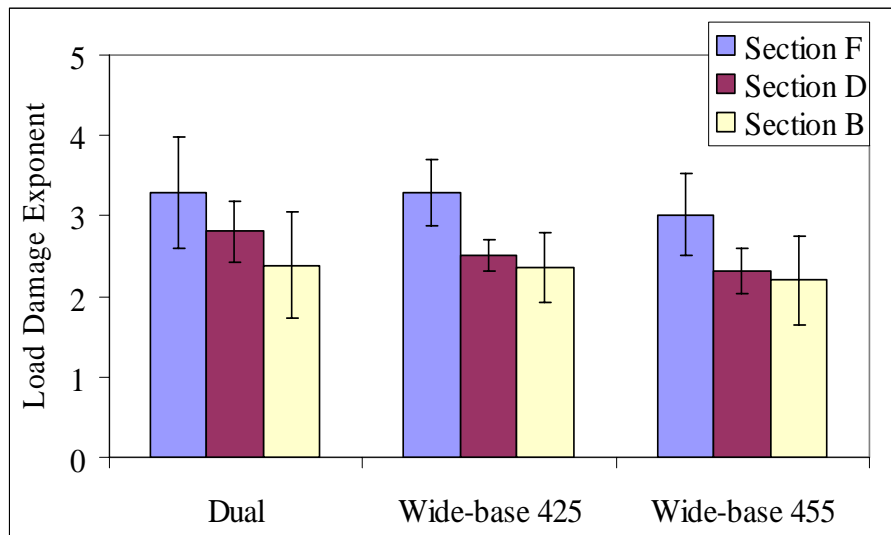
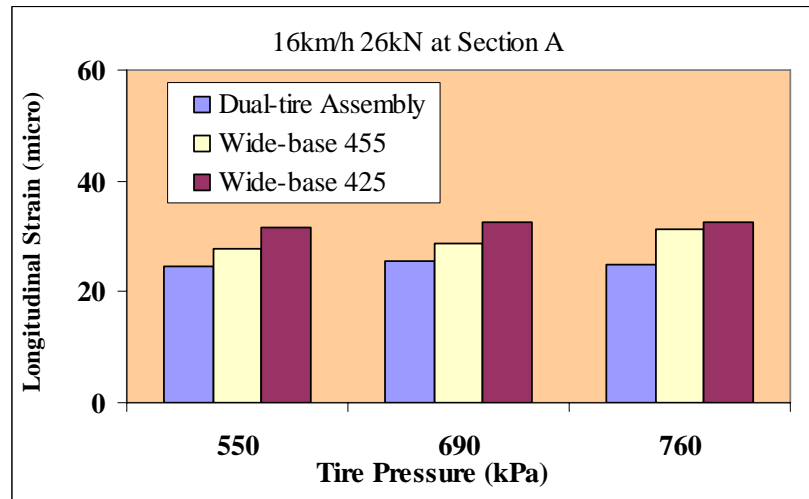


FIGURE 8 Load damage exponents for different pavement sections.

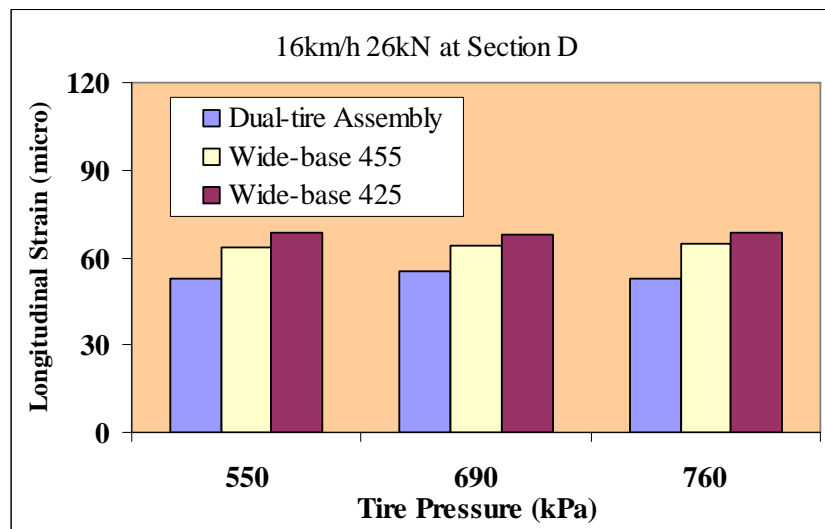
4.5 Effect of Tire Pressure

Currently, there is a growing concern over the increase in tire pressures that are believed to contribute to the increase in pavement damage. Since the AASHTO Road Test, the average inflation pressure has risen from 550 to 760kPa to accommodate for the increased load limits and replacing bias ply tires by radial ply tires (10). As shown in

Figure 9, the measured pavement response is not significantly affected by the increase of tire inflation pressure from 550 to 760kPa at Sections D and A. It was consistent with the previous research finding that for a thick HMA layer, the pavement's bottom-up fatigue was clearly controlled by load and not by tire inflation pressure. An increase in tire pressure had a pronounced effect on thin flexible pavement sections; the effect diminishes with HMA thickness increase. The tire pressure mainly affects the upper 50mm of the HMA (11).



(a)



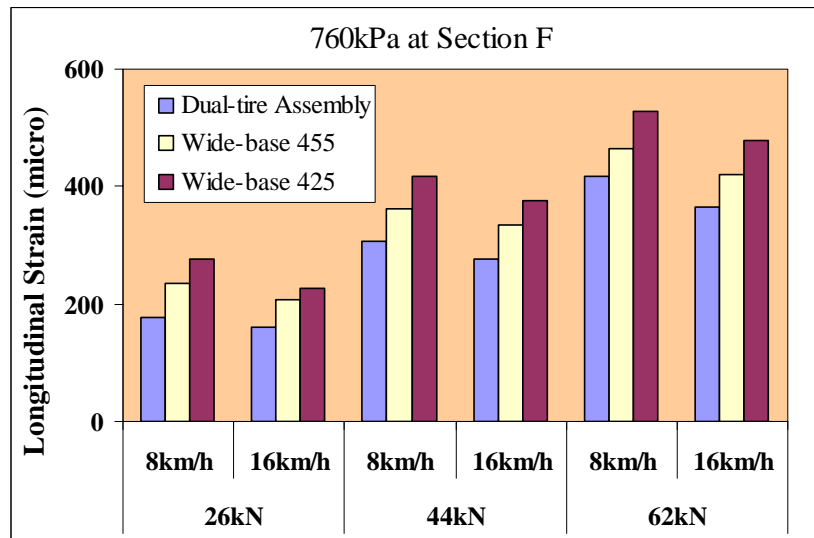
(b)

FIGURE 9 Measured strains under inflation pressure for (a) section A and (b) section D.

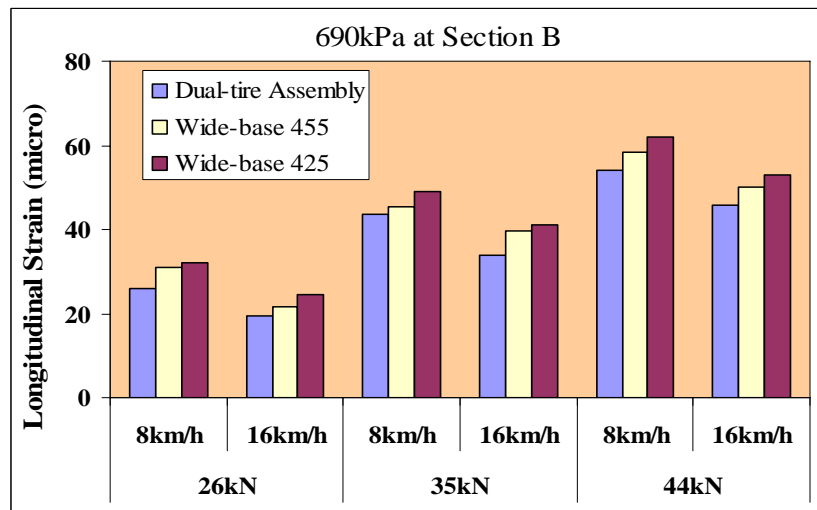
4.6 Effect of Vehicle Speed

As shown in Figure 10, the speed has a significant effect on measured pavement response. When the speed increases from 8km/h to 16km/h, the tensile strains at the bottom of the HMA layer in all four sections apparently decrease. This is due to two

reasons: 1) when the speed increases, the time of contact between the tire and the pavement decreases; and 2) because HMA is a viscoelastic material, it has a smaller modulus under lower loading frequency (lower speed). The effect of dynamic loading is neglected because the tire load is applied on the pavement without a suspension system. In real traffic, the pavement response is dependent upon the combined influence of moving speed and dynamic loading amplitude and frequency (12). Al-Qadi and Yoo (2007) showed that at low temperature, high speed could induce higher strain in the pavement (13).



(a) Section F



(b) Section B

FIGURE 10 Measured strains under different speeds for (a) Section F and (b) Section B.

It has to be noted that a recent study by Al-Qadi et al. (14, 15) reported that flexible pavement damage potential might be caused by different parameters than the ones currently used in the empirical-mechanistic fitting models for flexible pavement

damage prediction. Alternative parameters that are potentially responsible for the flexible pavement damage include vertical shear strains within the HMA layer. At intermediate to high temperatures, the vertical shear strains at the shallow depth (up to 100mm below the surface) are significantly greater than the critical transverse and longitudinal tensile strains at the surface and bottom of HMA. This introduces a new phenomenon of crack development known as “near-surface” fatigue cracking. Therefore, although this study evaluates the potential fatigue damage as suggested by the AASHTO M-E design guide, the authors believe that near-surface cracking is more critical than bottom-up cracking for perpetual pavements.

5. Summary

This study investigated the effect of various loading parameters on measured tensile strain at the bottom of HMA. The following findings are based on the test data analysis:

- The Wide-base 425 tire exhibits the highest longitudinal strain and fatigue damage potential; while dual-tire assembly exhibits the lowest at the bottom of HMA layer. However, the difference in strain responses due to wide-base tires and dual-tire assembly diminishes as HMA thickness increases. The average peak longitudinal tensile strain ratios between wide-base tire and dual-tire assembly are 1.25 for wide-base 425 and 1.16 for wide-base 455.
- As would be expected, longitudinal strain increases almost linearly with load, and decreases as speed increases. The effect of tire pressure on the longitudinal strains under the bottom of HMA is negligible. The HMA layer thickness in this study is 152mm and greater. However, tire pressure may have an effect on the upper 50mm of the HMA layer.
- The effect of load on fatigue life is expressed as an exponential function. The damage exponents were found to be in the range of 1.7-3.3 for full-depth flexible pavement. The parameter depends on pavement thickness and tire configuration. However, it is the opinion of the authors that near- surface cracking caused by shear is more critical than tensile strain at the bottom of HMA for perpetual pavements. Hence, fatigue damage may not be determined using empirical equations that utilize tensile strain at the bottom of HMA layer for perpetual pavement.

Acknowledgement

This publication is based on the results of ICT-R59, *Evaluation of Pavement Damage Due to New Tire Designs*. ICT-R59 is conducted in cooperation with the Illinois Center for Transportation; the Illinois Department of Transportation, Division of Highways; and the U.S. Department of Transportation, Federal Highway Administration. The authors would like to acknowledge David Lippert’s support of the wide-base tire research and the assistance of the following members of the Technical Review Panel for ICT-R59: Mark Gawedzinski (Chair), Amy Schutzbach, Bruce Peebles, Charles Wienrank, and Rich Telford. The authors would like also to acknowledge their colleagues Samer Dessouky

and Jim Meister for their help in accelerated loading testing and data management. The contents of this paper reflect the view of the authors, who are responsible for the facts and the accuracy of the data presented herein. The contents do not necessarily reflect the official views or policies of the Illinois Center for Transportation, the Illinois Department of Transportation, or the Federal Highway Administration. This paper does not constitute a standard, specification, or regulation.

References:

1. Cost 347, *Improvements in Pavement Research with Accelerated Load Testing*, European Cooperation in the field of Scientific and Technical Research. 2004
2. Tabatabaee, N., I. L. Al-Qadi, and P. E. Sebaaly, Field Evaluation of Pavement Instrumentation Methods, *Journal of Testing and Evaluation*, ASTM, Vol. 20, No. 2, March 1992, pp. 144-151.
3. Baker, H. B., M. R. Buth, and D. A. Van Deusen, *Minnesota Road Research Project: Load Response Instrumentation Installation and Testing Procedures*. Final Report, No. MN/PR-94/01, Minnesota Department of Transportation, St. Paul, 1994
4. WesTrack Team, *Accelerated Field Test of Performance-Related Specifications for Hot-Mix Asphalt Construction*, Final Report for Contract No. DTFH61-94-C-00004, Reno, Nev., 1996
5. Al-Qadi, I. L., A. S. Lahouar, G. W. Flintsch, and T. E. Freeman, Quantitative Field Evaluation and Effectiveness of Fine Mix under Hot-Mix Asphalt Base in Flexible Pavements, In *Transportation Research Record*, No.1823, TRB, National Research Council, Washington, D.C., 2003, pp. 133-140
6. Garcia, G. and M. Thompson, *Validation of Design Concepts for Extended Life Hot Mix Asphalt Pavements*, IHR-R39 Project Review, 2004.
7. Al-Qadi, I. L., M. A. Elseifi, and P. J. Yoo, Characterization of Pavement Damage Due to Different Tire Configurations, *Journal of the Association of Asphalt Paving Technologists*, Vol. 74, 2005, pp. 921-962.
8. Chen D. H., E. R. Cortez, F. Zhou, W. Yang, and K. Petros, Analysis of Overload Damages in Thin Flexible Pavements, Paper #06-0391, *Proceeding of TRB 85th Annual Meeting*, Washington, D.C., January 22-26, 2006
9. ARA, Inc., ERES Division, *Development of the 2002 Guide for the Design of New and Rehabilitated Pavements*, NCHRP 1-37A, TRB, National Research Council, Washington, D.C., 2004.
10. Gillespie, T. D., S. M. Karimihas, D. Cebon, M. W. Sayers, M. A. Nasim, W. Hansen, and N. Ehsan, *Effects of Heavy-vehicle Characteristics on Pavement Response and Performance*, In NCHRP Report 353, TRB, Washington D.C., 1993
11. Siddharthan, R. V., Investigation of Tire Contact Stress Distributions on Pavement Response, *Journal of transportation Engineering*, Vol. 128, 2002, pp. 136-144

12. Cebon, D., Road Damaging Effects of Dynamic Axle Loads. Proceedings of the *International Symposium on Heavy Vehicles Weights and Dimensions*, Kelowna, British Columbia, Canada, 1986, pp. 37–53.
13. Yoo, P. J. and I. L. Al-Qadi, Effect of Transient Dynamic Loading on Flexible Pavements, In *Transportation Research Record*, No.1990, TRB, National Research Council, Washington, D.C., 2007 (b). pp. 129-140
14. Al-Qadi, I. L., H. Wang, P. J. Yoo, and S. H. Dessouky, Dynamic Analysis and In-Situ Validation of Perpetual Pavement Response to Vehicular Loading, Accepted for publication in *Transportation Research Record*, Paper No. 08-0612, TRB, National Research Council, Washington, D.C., 2008 (a)
15. Yoo, P. J. and I. L. Al-Qadi, Fatigue Crack Potential in Hot-Mix Asphalt from Three Dimensional Tire-Pavement Contact Stresses, Accepted for publication in *Journal of Association of Asphalt Paving Technologists*, Vol. 77, 2008(b)